Journal of Cleaner Production 418 (2023) 138158

Contents lists available at ScienceDirect

Journal of Cleaner Production

journal homepage: www.elsevier.com/locate/jclepro

Leaf surface functional traits influence particulate matter and polycyclic aromatic hydrocarbons air pollution mitigation: Insights from Mediterranean urban forests

Antonello Prigioniero [a,1], Alessia Postiglione [a,1], Daniela Zuzolo [a,*], Ülo Niinemets [b], Maria Tartaglia [a], Pierpaolo Scarano [a], Mariano Mercurio [a], Chiara Germinario [a], Francesco Izzo [c], Marco Trifuoggi [d], Maria Toscanesi [d], Rosaria Sciarrillo [a], Carmine Guarino [a]

[a] *Department of Science and Technology, University of Sannio, via de Sanctis snc, Benevento, 82100, Italy*
[b] *Institute of Agricultural and Environmental Sciences, Estonian University of Life Sciences, Kreutzwaldi 1, Tartu, 51006, Estonia*
[c] *Department of Earth Sciences, Environment and Resources, University of Naples Federico II, via Cintia, Naples, 80126, Italy*
[d] *Department of Chemical Sciences, University of Naples Federico II, via Cintia, Naples, 80126, Italy*

ARTICLE INFO

Handling Editor: Giovanni Baiocchi

Keywords:
Air phytoremediation
Cuticle
Functional Traits
Nature-based solutions
PAH
Particulate matter
Stomata
Trichomes

ABSTRACT

In this work the leaf surface functional traits, potentially useful for air phytoremediation of particulate matter (PM) and polycyclic aromatic hydrocarbons (PAH), of 28 woody species have been characterized, and the role of these stomata, trichomes and cuticle traits in phytoremediation have been assessed looking at existing correlations with species-specific ability to sequester and retain airborne pollutants. Leaves were sampled in urban area in August and September and functional traits were measured using Scanning Electron Microscopy and Fourier-transform infrared spectroscopy. Pollutants were extracted by leaves and their concentrations and daily uptake rates were measured using gas chromatography. Significant differences were found between species in the arrangement of functional traits, concentrations and daily uptake of pollutants. Correlations between variables were studied by means of principal component analysis. The trichomes-related traits scaled positively with PM concentration daily uptake, whereas for PAH air phytoremediation, the cuticle physical and chemical features are relevant. Trichomes increase the leaf area several fold providing extra surfaces for PM retention, while cuticle thickness and esterification regulate the PAH retention and translocation in subcuticular tissues. Results provide novelty on the relationships between leaf surface functional traits and plant species phytoremediation potential, outlining an innovative way of measuring leaf surface functional traits. In addition to broadening the economic spectrum of functional traits, it is emphasized how important leaf surface functional traits are in the nature-based solutions definition and planning.

1. Introduction

The past decade has seen a consistent increase in studies on pollutant concentrations in urban areas, sources and effects on human health (Kampa and Castanas, 2008; Landrigan, 2017). Particulate matter (PM) is of particular concern for human health (Anderson et al., 2012; Losacco and Perillo, 2018). The peculiar composition of PM, coarse (PM_{10}) or fine ($PM_{2.5}$), makes it one of the most dangerous pollutants because it remains in suspension in the air for a long time leading the human population to chronic exposure causing cytotoxicity and genotoxicity manifesting in respiratory and cardiac disorders and diseases (Forbes et al., 2009; Hamanaka and Mutlu, 2018). PM composition depends on the origin of particles and ambient air chemistry, and the health risks of PM can be similar to polycyclic aromatic hydrocarbons (PAH) (Chen et al., 2021; Yang et al., 2021). PAH are known to play an important role as persistent and hazardous PM-related air contaminants (Brook et al., 2010). Based on their molecular mass, PAH can be grouped as: low (LMM), medium (MMM) and high molecular mass (HMM) PAH with different physico-chemical properties and environmental hazard (Brazkova & Krastanov, 2013; Mihankhah et al., 2020).

* Corresponding author.
E-mail address: dzuzolo@unisannio.it (D. Zuzolo).
[1] Equal contribution.

https://doi.org/10.1016/j.jclepro.2023.138158
Received 11 May 2023; Received in revised form 30 June 2023; Accepted 17 July 2023
Available online 18 July 2023

Urban forests are one of the main nature-based solutions (NBS) for reduction of PM and its impacts on human wellbeing (Marando et al., 2016; Cariñanos et al., 2017). Canopies of urban trees and shrubs provide regulation ecosystem services retaining pollutants on their leaf surfaces or incorporating them into their tissues (Nowak et al., 2014; Blanusa et al., 2015; Livesley et al., 2016; Łukowski et al., 2020).

Although numerous studies have been conducted to identify the relationship between urban vegetation and air pollution mitigation, very few have focused on the specific removal capacity. Thus, it remains uncovered to which extent air pollutants removed by trees are related to the specific functional traits of leaf surface. Moreover, the number of modelling-based studies is far greater than direct empirical ones (Gómez-Moreno et al., 2019). A review on urban vegetation and air pollution by Janhall (2015) suggests that large experimental datasets are needed to upgrade existing models, including a detailed description of the parameters that influence the effects of vegetation on air pollution. Leaves provide a surface with chemical and microscopic features that vary from species to species, altering the capacity for pollutants removal (Terzaghi et al., 2013). Functional traits that can affect the pollutant retention capacity include all microscopic structures capable of providing adhesion and retention such as structural and physico-chemical traits of the cuticle, traits that increase surface area for uptake and adsorption such as trichomes, protruding epicuticular waxes, cell wall extrusions, and traits that scale with uptake into leaf interior including size, density and openness of stomata and cuticle permeability (Niinemets et al., 2014; Mukherjee and Agrawal, 2018; Gaglio et al., 2022). Leaf cuticle thickness, hydrophobicity and porosity appear to be the main features involved in the phytoremediation of pollutants such as PM and organic molecules such us PAH (Jouraeva et al., 2003; Li et al., 2017). The stomata play a dual role in phytoremediation. They provide an entry route for pollutants, but at the same time they provide discontinuities on the leaf surface, whose shape, arrangement and surface can influence the phytoremediation capacity (Samson et al., 2017; Baraldi et al., 2019). Stomata can also have hydrophilic regions that could serve as sites of deposition of hydrophilic pollutants (Burkhardt, 2010). Non-glandular trichomes provide complexity to the leaf surface and function as traps for particulate pollutants whose retention performance depends on density, size but also shape (Grote et al., 2016; Baraldi et al., 2019). Thus, the functional traits of leaves of individual species are expected to provide an integrated measure for the pollutant deposition capacity of the leaf surface, but there is stilllimited information about the interspecific variability in pollutants deposition capacity and of how the deposition capacity depends on key leaf surface traits. In fact, traits like trichome surface area per leaf surface area and stomatal area and stomatal pore area per leaf area and cuticular traits have seldom been assessed and as the result, assessment of the vegetation air remediation capacity is bound to large uncertainties.

Based on these considerations, we believe that expanding information on the relationship between leaves plant functional traits and air pollutant mitigation is critical to improving numerical modeling related to air phytoremediation. In this study, we focused on Mediterranean ecosystem which is very specific due to the extensive summer drought, extension of the growing season due to moderately low winter temperatures and abundant rainfall. Hence, in Mediterranean ecosystemthe plants adapted e often show evergreen sclerophyllous leaves with peculiar traits which role in retention of pollutants is of interest and is worthy of further exploration (Yadav et al., 2004; Niinemets, 2010; Niinemets and Keenan, 2014; La Riva et al., 2018).

The specific aims of this study were: (i) characterization of leaf surface functional traits of tree species commonly used for ornamental purpose in Mediterranean urban forests; (ii) exploration of the relationships of leaf concentrations and daily uptake rate of PM and PAH with leaf surface functional traits in the observed species with contrasting leaf characteristics.

We hypothesized that adsorption of different pollutants scales positively with trichome surface area, adsorption and cuticular uptake of more hydrophobic pollutants with surface hydrophobicity and cuticle thickness. To test these hypotheses, we related plant pollutants (PM10, PM2.5 and PAH) accumulation with leaf surface features (the stomatal and trichome surface areas and numbers per leaf area, the degree of cuticle esterification, and cuticle thickness) for 28 widespread woody species widely used for ornamental purposes in Mediterranean cities.

2. Materials and methods

2.1. Sampling sites

A double sampling campaign was carried out in the city center of Naples (Southern Italy) to investigate the capacity of plant species to accumulate air pollutants (PM10, PM2.5 and PAH) from urban air by leaves of 28 widespread ornamental woody species in the area (Fig. 1, Table S1 in SM). The chosen sampling areas (40°50′ N 14°15′ E, 17 m.a.s.l.) has a Köppen subtype Csa climate (Kottek et al., 2006) and is characterized by high anthropogenic air pollutant emissions (Fortelli et al., 2016). Sampling sites were selected considering their proximity to the main and busiest squares and streets in the city center, and their proximity to meteorological and air quality monitoring stations of the Campania Regional Agency for Environmental Protection (ARPAC) (Fellet et al., 2016, Fig. 1). Sampling was performed on August 1st, 2019 (D_0) and on September 1st, 2019 (D_1). During the two campaigns, leaf tissue from the 28 investigated tree species was collected. A minimum of three to a maximum of ten individuals per species were chosen depending on the plants availability at the sampling points. From each tree, up to 15 leaves were randomly selected at least three different branches facing the street, at a maximum height of 2 m above the ground. Leaves from individuals of the same species, sampled at the same sampling point, were mixed to reduce intraspecific variability. Sub-samples were extracted from each pool for triplicate analysis.

2.2. Characterization of leaf functional traits

The leaf surface functional traits investigated were the physical and chemical characteristics of trichomes, cuticle and stomata as defined with the corresponding acronyms in Table S2 in SM. Three leaves of each species were randomly selected from the sub-samples and analyzed. Number of stomata and trichomes on both leaf surface ($N_{s,u}$, $N_{s,l}$, $N_{t,u}$, $N_{t,l}$), surface area of stomata, stomatal pores and trichomes per unit leaf surface area, ($S_{s,u}$, $S_{s,l}$, $S_{sp,u}$, $S_{sp,l}$, $S_{t,u}$, $S_{t,l}$) and cuticle thickness ($T_{c,u}$, $T_{c,l}$) were estimated on five randomly-selected points on each leaf by scanning electron microscope (SEM) image acquisition and analysis. Liquid removal from leaf specimens was carried out by critical point drying with liquid CO_2 in a K-850 Critical Point Dryer (Quorum Technologies, Laughton, UK). The samples were further mounted on aluminum specimen stubs with double-sided tape and coated with gold using a Q150R ES Sputter Coater (Quorum Technologies, UK). Finally, they were observed via Scanning Electron Microscopy (SEM, Zeiss EVO 15 HD VPSEM) operating at 10 or 15 kV accelerating voltage to record images. To observe and record the number and surface of stomata and number of trichomes, the specimens were mounted exposing upper and lower leaves surface. To investigate cuticle thickness and trichome surface, cross sections of leaves were mounted on stubs. The presence of protruding veins was used to distinguish between the two sides.

The chemical properties of the cuticle were analyzed by Fourier-transform infrared spectroscopy (FTIR). From these measurements, the esterification indices for upper and lower leaf surface (E_u, E_l) were obtained from the ratio between the absorbance intensity of the stretching vibration of esters and the asymmetric stretching vibration of methylene (Prigioniero et al., 2022). Esterification index characterizes the degree of cross-linkage of cutin forming hydroxy- and peroxyacids (Heredia-Guerrero et al., 2014).

For hairy leaves, we found five different trichome shapes: stellate trichomes (found in *Q. ilex*), dendritic trichomes (found in *P.* ×

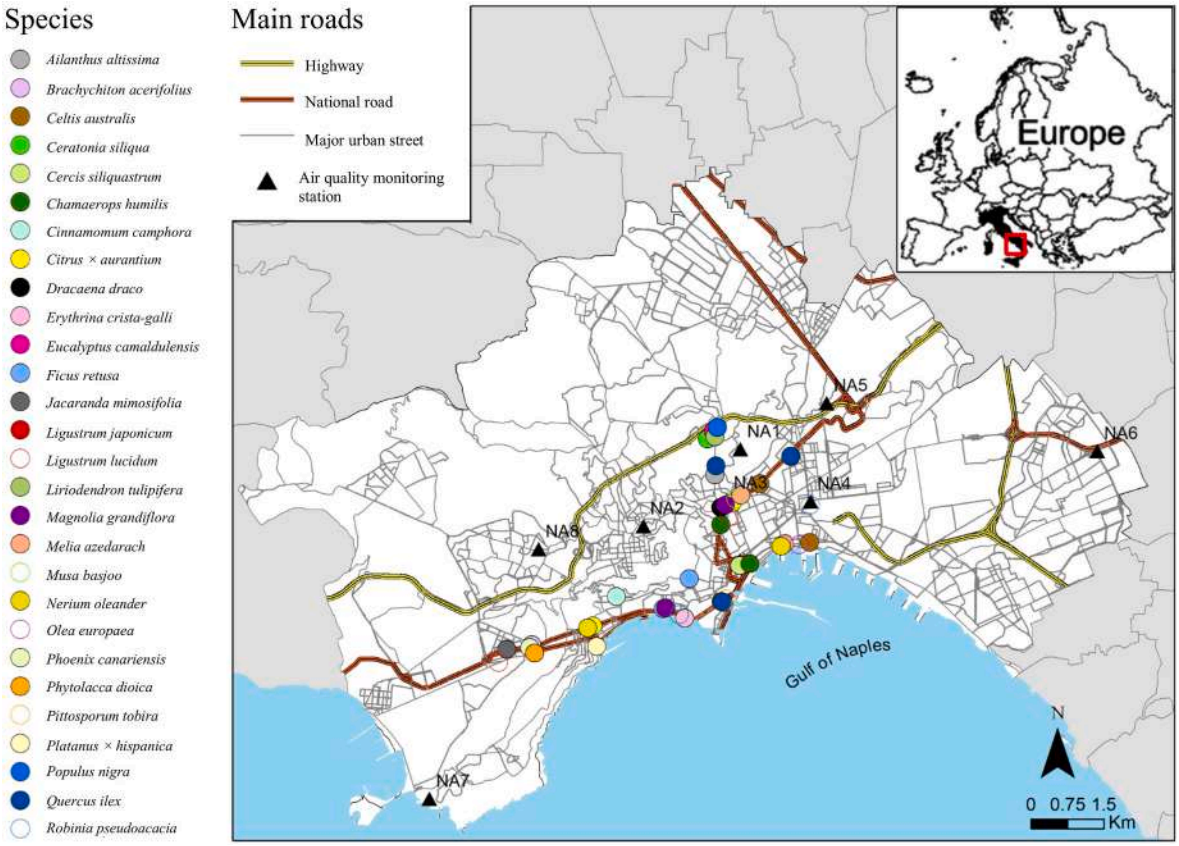

Fig. 1. Sampled plant species, and the study area with sampling points, air quality monitoring stations, and road network (Naples, Southern Italy).

hispanica), peltate trichomes (found in *O. europaea* samples), cylindrical trichomes (found in *C. humilis*) and conical trichomes (found in the remaining species with hairy leaves, Fig. 2). We calculated the total trichome surface area per leaf area, (S_t, m^2 m^{-2}) with simple geometric approximations (Equation S1–S5 in SM).

2.3. Pollutant concentrations (C) and uptake rates (U)

The leaf surface concentrations (C) at each sampling date (D_0 and D_1) of fine ($C_{PM2.5,\ D0}$, $C_{PM2.5,\ D1}$) and coarse particulate matter ($C_{PM10,\ D0}$, $C_{PM10,\ D1}$), and the share of hydrophobic coarse and fine particulate matter (Θ_{PM10} and $\Theta_{PM2.5}$; ratio of PM_{10} and $PM_{2.5}$ amounts in leaf

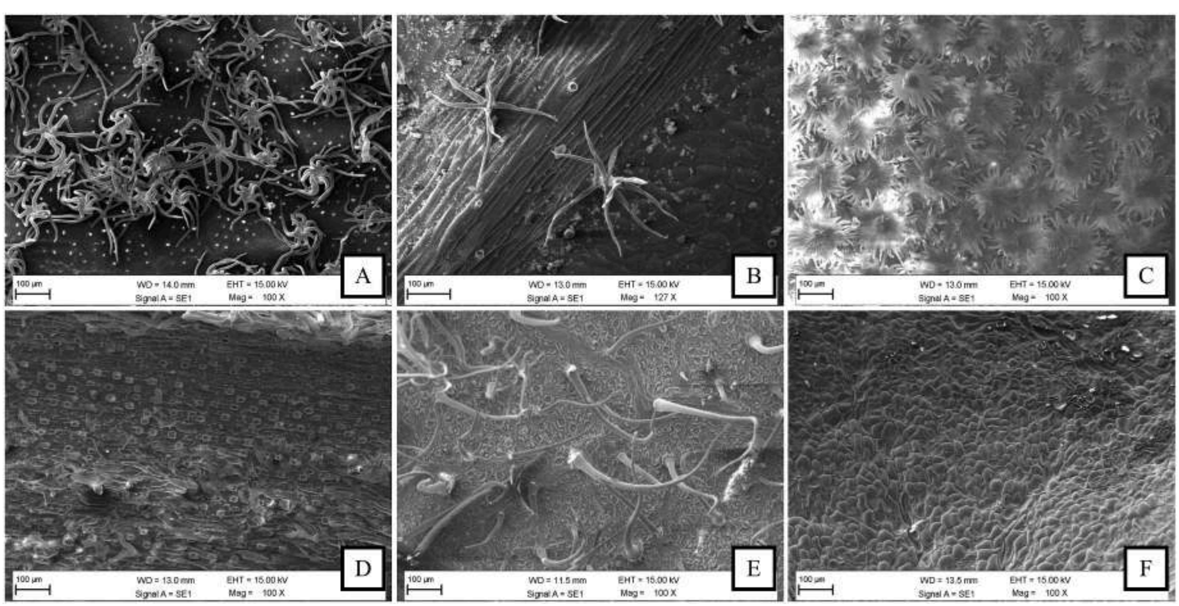

Fig. 2. Representative examples of trichome morphologies found on leaf lower surfaces: (A) *Quercus ilex* stellate trichomes, (B) *Platanus* × *hispanica* dendritic trichomes, (C) *Olea europaea* peltate trichomes, (D), *Chamaerops humilis* cylindrical trichomes, (E) *Celtis australis* conical trichomes, (F) *Cercis siliquastrum* glabrous leaf surface. The images were acquired via Scanning Electron Microscopy (SEM).

chloroform extracts relative to sum of the amounts in chlorophorm and distilled water extracts) (Tables S7 and S8 in SM) were determined washing the same amount of leaf area per species (400 cm^2) with distilled water first, and chloroform later, and then vacuum-filtering the resulting washing solutions using previously weighed filters of different porosity (Prigioniero et al., 2022). The concentrations of low, medium and high molecular mass PAH at each sampling date in intact leaves and dewaxed leaves (after chloroform washes) were determined gas chromatographically Once the concentrations of each pollutant were obtained at the two sampling dates (C_{D0} and C_{D1}), the uptake rate (U) was estimated as follow:(Prigioniero et al., 2022).

$$U = \frac{(C_{D1} - C_{D0})}{\Delta t} \quad \text{Equation 1}$$

2.4. Data analyses

Data were statistically analyzed with R ver. 4.2.2 (R Core Team, 2015) to perform analysis of variance (ANOVA) followed by Tukey's Honest Significant Difference (HSD) post-hoc test to separate differences between species in U and C. One-way multivariate analysis of variance (one-way MANOVA) using Pillai's trace criterion was used to test for differences between species in leaf functional traits. Correlation analysis was used to examine the dependencies of C and U on characteristics of trichomes, cuticle and stomata. All statistical tests were considered significant at $p < 0.05$. Finally, two-dimensional PCA biplots were generated to distinguish the main patterns in the dataset (Wickham, 2016), in particular, to determine how the analyzed samples, belonging to different tree species, group according to their species-specific functional traits and pollutant accumulation capacities The PCA biplot is a 2D graphical representation that shows associations between observations (plant samples) and the traits. The lengths of the rays (vectors) are directly proportional to the variance of the corresponding variable included in the two components displayed, while the angle between the vectors indicate the strength of correlation between them (Zuzolo et al., 2020).

3. Results

3.1. Leaf surface functional traits

Among the 28 studied species, the number of stomata on the lower leaf surface ($N_{s,\ l}$) varied 12.03-fold from $6.54 \cdot 10^7$ m^{-2} in *P. nigra* to $7.87 \cdot 10^8$ m^{-2} in *C. australis* (Table S5 in SM, Fig. 3). The stomatal surface area per lower leaf surface area ($S_{s,\ l}$) varied 13.13-fold from 0.015 m^2 m^{-2} to 0.197 m^2 m^{-2} and stomatal pore area per lower leaf surface area ($S_{sp,\ l}$) 11.50-fold from 0.002 m^2 m^{-2} to 0.023 m^2 m^{-2} (Table S5). *Magnolia grandiflora* had the highest stomatal area per lower leaf area, followed by *B. acerifolius*, and stomatal pore area per lower leaf area was the greatest in *B. acerifolius* and *C. camphora* (Table S5). Only four species were amphistomatous with stomata on both the lower and upper sides. These four species ranked according to the number of stomata per upper leaf area ($N_{s,\ u}$) as follows: *P. canariensis* > *E. camaldulensis* > *E. crista-galli* > *D. draco* (Table S5, Fig. 3). Among the amphistomatous species, *E. camaldulensis* and *E. crista-galli* had a comparable number of stomata on both surfaces; the stomatal density for the lower-side was greater than that for the upper side in *D. draco*, and it was the opposite in *P. canariensis* (Table S5). *Phoenix canariensis* was the species with the highest values for both functional traits ($S_{s,\ u} = 0.050$ m^2 m^{-2}; $S_{sp,\ u} =$ 0.009 m^2 m^{-2}), (Table S5). The lowest values for both functional traits were observed in *D. draco* ($S_{s,\ u} = 0.003$ m^2 m^{-2}; $S_{sp,\ u} = 3.40.10^{-4}$ m^2 m^{-2}) (Table S5).

Regarding the cuticle thickness of the upper leaf side ($T_{c,\ u}$), *O. europaea showed the highest one* ($T_{c,\ u} = 10.8$ μm), and similar values were observed in *N. oleander*, *M. grandiflora*, *Q. ilex* and *D. draco* (Table S5, Fig. 4). The species with the thinnest cuticle on the upper side of the leaf (Tc, u) were *P. nigra*, *P. dioica* and *M. azedarach* (Table S5). Turning to the lower cuticle ($T_{c,\ l}$), a variation of 3.92-fold with a range from 1.97 μm to 7.72 μm was found (Table S5). The thickest lower leaf cuticle was found in *D. draco* (Table S5). The ATR-FTIR analysis of leaf surfaces indicated that the position (wavenumbers) of the main absorption bands in the infrared spectra were similar across species (Fig. S1 in SM). However, relative intensities of different absorption bands had species-specific signatures (Fig. S1). The esterification index for lower leaf side (E_l) ranged from 0.09 to 0.71, and that for upper leaf side (E_u) from 0.10 to 0.58 (Table S5). *Quercus ilex* and *J. mimosifolia* had the highest E_l values, and *R. pseudoacacia* and *P. canariensis* the lowest values (Table S5). *Jacaranda mimosifolia* and *A. altissima* had the highest E_u values, and *P. canariensis* the lowest value (Table S5).

Most of the tree species sampled had glabrous leaves, and only ten species had trichomes (Table S5). Nine species had trichomes on lower leaf surface ($N_{t,\ l}$, m^{-2}), *C. humilis* had the highest $N_{t,\ l}$ and *P.* × *hispanica* had the lowest value (Table S5). *Quercus ilex* had stellate trichomes and the greater complexity of trichomes was reflected in the highest trichome area per leaf area ($S_{t,\ l,} = 8.10$ m^2 m^{-2}, Table S5). Among the species with trichomes on the lower leaf surface, four also had trichomes on the upper surface, and in addition, *A. altissima* had trichomes exclusively on the upper surface (Table S5). These five species ranked according to $N_{t,\ u}$ as *C. australis* = *R. pseudoacacia* > *N. oleander* > *O. europaea* > *A. altissima* (Table S5). *Celtis australis* and *O. europaea* had the highest trichome surface area per upper leaf surface area ($S_{t,\ u}$), and *N. oleander* the lowest $S_{t,\ u}$ (Table S5).

3.2. Environmental pollution and weather conditions

PM concentration levels in the air were similar for each sampling date during the entire exposure period (coefficient of variation (Thangjai et al., 2021) < 36.5%; Tables S6 and S7 in SM). Therefore, average concentration of pollutants was used to characterize air pollution conditions over the entire period for each ARPAC station (www.arpacampania.it). The monthly average (±SD) temperature was 27.4 ± 1.1 °C, the average (±SD) wind speed was 2.8 ± 0.05 m s^{-1}, the main wind direction was west, and there was no precipitation during the entire period.

3.3. Pollutant concentrations and accumulation rates

3.3.1. Particulate matter

The total amount of coarse particulate matter (PM_{10}; sum of distilled water and chloroform extracts) observed on the first sampling event on 1st August (D_0) varied 161.28-fold, and the species ranked as: *D. draco* > *P. canariensis* > *Q. ilex* = *E. camaldulensis* (Table S8 in SM). On the second sampling event on 1st September (D_1), total PM_{10} concentration varied 27.33-fold, and the species showing the highest values were *O. europaea* and *C. humilis* (Table S8). *Chamaerops humilis* and *O. europaea* also showed the greatest values of daily uptake rate of coarse particulate matter (U_{PM10}) (Table S8). However, several species were not able to increase PM_{10} concentrations (zero U_{PM10} values, Table S8). Θ_{PM10} varied 31.76-fold, with the highest values in *E. camaldulensis*, *P. dioica* and *P. nigra*, and the lowest value in *D. draco* (Table S8).

The total concentration of $PM_{2.5}$ on D_0 varied 26.23-fold, with the highest values in *M. grandiflora*, *P. canariensis* and *A. altissima* (Table S9 in SM). On D_1, total $PM_{2.5}$ concentration varied 77.43-fold, and *O. europaea* and *E. crista-galli* had the highest concentration of fine particulate matter (Table S9). Leaves of *O. europaea, E. crista-galli, M. azedarach* and *F. retusa* had the highest $U_{PM2.5}$ value, while no uptake was detected in several species (Table S9). $\Theta_{PM2.5}$ varied 8.64-fold, and the species with the highest $\Theta_{PM2.5}$ were *E. crista-galli, E. camaldulensis* and *P. nigra* (Table S9).

3.3.2. Polycyclic aromatic hydrocarbons in intact and dewaxed leaves

In August (D_0), the average values of LMM PAH did not differ among

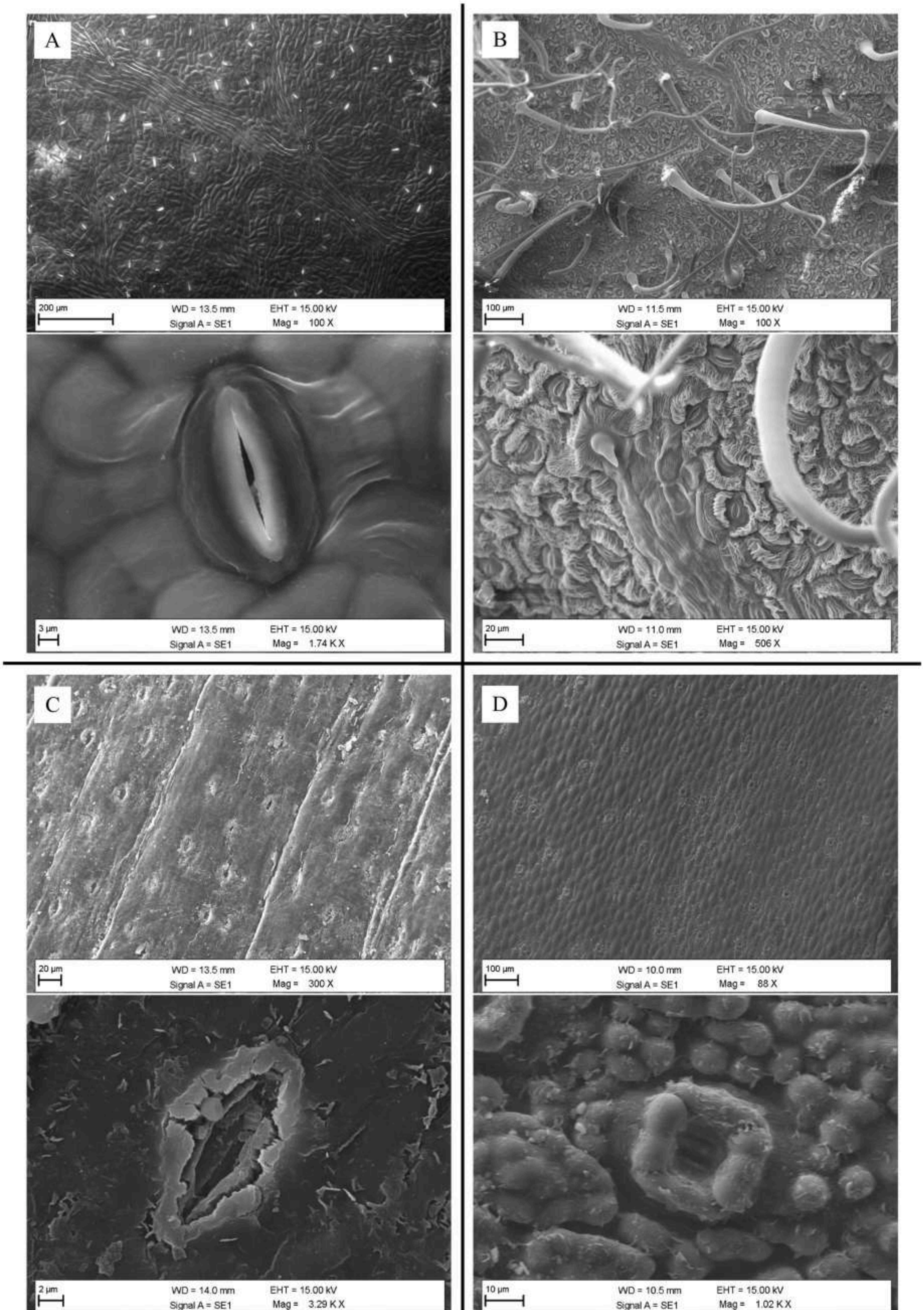

Fig. 3. Representative examples of stomata distribution and details on (A) lower leaf side of *Populus nigra*, (B) lower leaf side of *Celtis australis*, (C) upper leaf side of *Phoenix canariensis*, (D) upper leaf side of *Dracaena draco*. Images were acquired with a Scanning Electron Microscope (SEM).

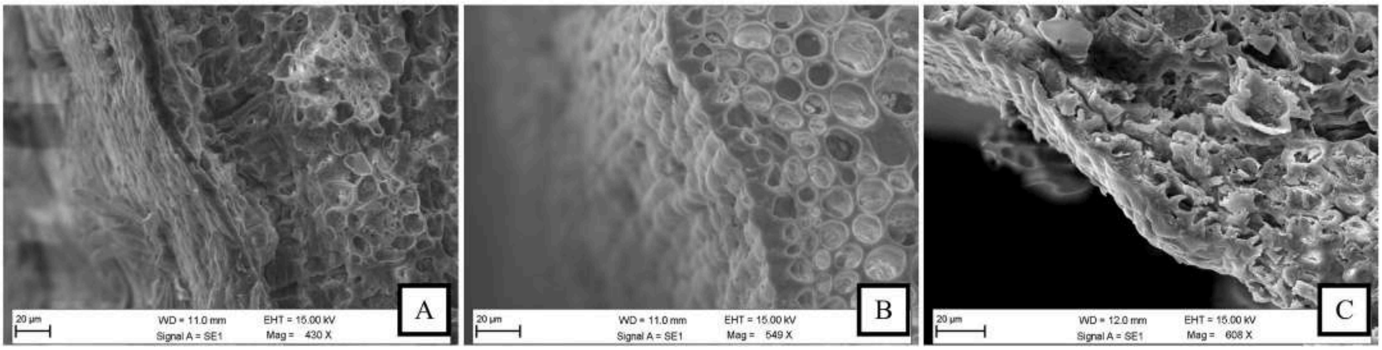

Fig. 4. Representative examples of cuticle layer of upper leaf side in (A) *Olea europaea*, (B) *Nerium oleander*, (C) *Quercus ilex*. Images were acquired with a Scanning Electron Microscope.

the species, and some species did not even show a detectable leaf LMM concentration (Table S10 in SM). After thirty days (D_1), LMM PAH concentrations varied 190-fold and *D. draco* had the highest concentration (Table S10). *Dracaena draco* had the highest $U_{\mathrm{LMM,i}}$ followed by *O. europaea* (Table S10). MMM PAH concentrations at D_0 varied 49-fold, and the highest concentrations were found in the samples of *C.* × *aurantium*, *L. lucidum*, *O. europaea* and *P. nigra* at D_0, and in leaves of *C.* × *aurantium*, *D. draco*, *L. japonicum* and *O. europaea* at D_1 (Table S10). *Ligustrum japonicum* and *D. draco* were the species with the $U_{\mathrm{MMM,i}}$ (Table S10). High molecular mass (HMM) PAH were found only in eight species at D_0, and only in ten species at D_1 (Table S10). The concentrations of HMM PAH in intact leaves ranged from 36.5 µg m^{-2} to 1529 µg m^{-2} at D_0 and from 22.3 µg m^{-2} to 1039 µg m^{-2} at D_1 (Table S10). The species showing the highest values was *E. crista-galli* (Table S10).

Analysis of dewaxed leaves provides information of the amount of PAH translocated into and accumulated in the subcuticular tissues and trichome hydrophilic regions over a 30-day period. Overall, the PAH concentrations in dewaxed leaves were low compared to those recorded for intact leaves, indicating that these pollutants accumulated mainly in the cuticular hydrophobic layer (Table S11 in SM). LMM PAH were found in higher concentrations in the cuticle-deprived leaves of *P. canariensis* in August, but in September the species showing higher amounts of these pollutants in their tissues were *P. tobira*, *N. oleander* and *M. azedarach*, also presenting the highest values of $U_{\mathrm{LMM,dw}}$ (Table S11). For MMM PAH, the concentration in dewaxed leaves in August ($C_{\mathrm{MMM},D0,\mathrm{dw}}$) was the greatest in *P. nigra* (Table S11). One month later ($C_{\mathrm{MMM},D1,\mathrm{dw}}$), the highest concentration was recorded for the leaves of *P. canariensis*, resulting in a daily uptake rate of one or two orders of magnitude higher in this species than in the others (Table S11). *Dracaena draco* was the species with the highest concentration of HMM PAH in the subcuticular tissues in August and September, but only for *M. azedarach* the value of $U_{\mathrm{HMM,dw}}$ exceeded the detection limit (Table S11).

3.4. Clustering of species according to functional traits and pollutant uptake

The two first axis of PCA altogether explained 49% of variance in the dataset (PC1 29.9% and PC2 19.1%). Different suites of functional traits clearly separated some of the studied species in the PCA space (Fig. 5). Upper leaf surface functional traits ($N_{\mathrm{s,\ u}}$, $S_{\mathrm{s,\ u}}$, $S_{\mathrm{sp,\ u}}$) determined the clustering of *E. crista-galli, E. camaldulensis* and *P. canariensis* samples

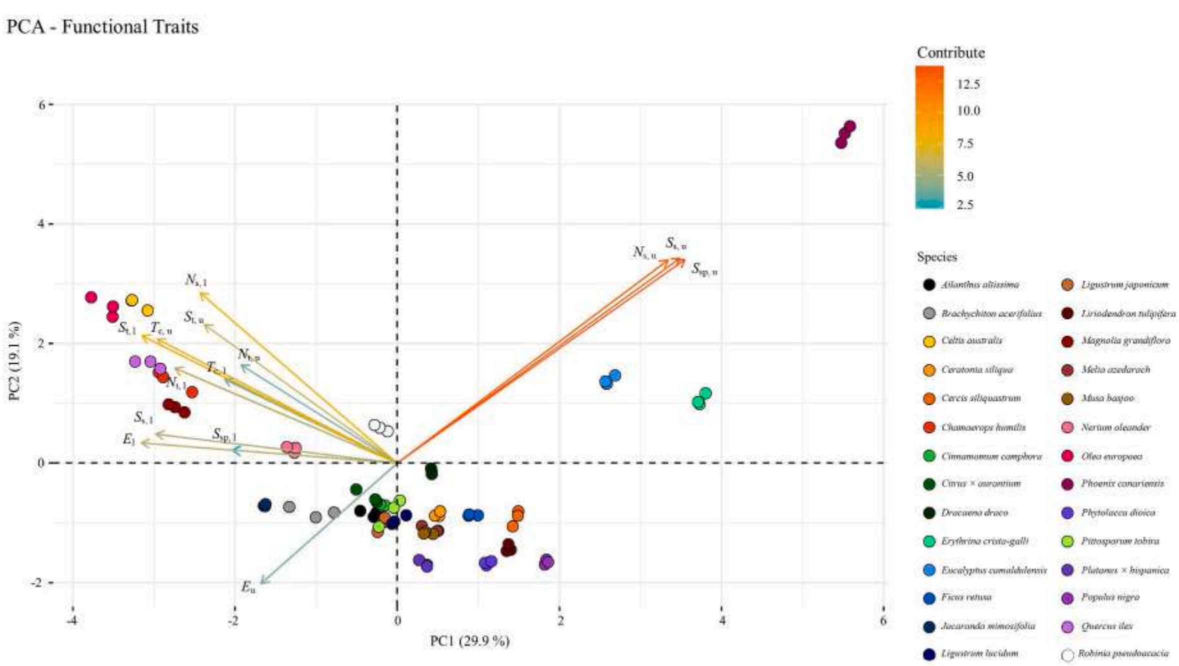

Fig. 5. Biplots of principal component analyses (PCA) showing the ordination of species in the PCA space as determined by leaf functional traits. Plant samples and the included variables are expressed as symbols and vectors. The plots display the first (PC1) and second (PC2) principal components, variance explained by PC1 and PC2 and the variable contributions (as characterized by the length of the vectors) to the first two principal components. All symbols are defined in Table S2.

(Fig. 5). These functional traits were opposite to E_u, which determines the clustering of the samples of *B. acerifolius*, *J. mimosifolia*, *C.* × *aurantium*, *A. altissima*, *C. camphora*, *P. tobira*, *L. lucidum* and *L. japonicum* (Fig. 5). The suite of traits projected on PC1 consisted of: E_l, $T_{c,\ l}$ and $T_{c,\ u}$, trichome traits on both surfaces ($N_{t,\ l}$, $N_{t,\ u}$, $S_{t,\ l}$ and $S_{t,\ u}$) and stomatal traits on the lower surface ($N_{s,\ l}$, $S_{s,\ l}$, $S_{sp,\ l}$). These traits clustered and separated *N. oleander, M. grandiflora, C. humilis, Q. ilex, O. europaea, C. australis* and *R. pseudoacacia* from the rest (Fig. 5). The remaining samples were well clustered by species, but not clearly separated by the variables used in this analysis (Fig. 5).

PCA based on surface functional traits and particulate matter and polycyclic aromatic hydrocarbon concentrations and uptake rates also resulted in SMmilar separation of species, accounting for the 46.5% of the total variance (PC1 28.5% and PC2 17.7%, Fig. 6). Upper leaf surface stomata related functional traits resulted positively correlated with Θ_{PM10} and $\Theta_{PM2.5}$, C and U of MMM PAH in dewaxed leaves and concentration of LMM PAH in dewaxed leaves, clustering *P. canariensis*, *E. crista-galli, E. camaldulensis* and *P. nigra* (Fig. 6). Θ_{PM10} grouped the samples of *F. retusa, L. lucidum, L. tulipifera* and *M. azedarach* (Fig. 6). Number and surface per lower leaf area of stomata ($N_{s,\ l}$, $S_{s,\ l}$, $S_{sp,\ l}$), esterification indices (E_l and E_u) and trichome number and surface per upper leaf area ($N_{t,\ u}$, $S_{t,\ u}$) only defined the samples of *C. australis* (Fig. 6). The uptake of coarse particles by leaves (U_{PM10}) was correlated with all trichome-related traits ($N_{t,\ u}$, $S_{t,\ u}$, $N_{t,\ l}$ and $S_{t,\ l}$) and the atmospheric concentrations of PM ($C_{PM10,\ a}$ and $C_{PM2.5,\ a}$); *Chamaerops humilis*, *Q. ilex*, *M. grandiflora* and *O. europaea* samples were grouped by these variables (Fig. 6). Cuticle thickness of both leaf sides was positively related to concentration of HMM PAH in dewaxed leaves ($C_{HMM,\ dw}$), concentration of coarse particulate matter (C_{PM10}), PAH concentration on intact leaves ($C_{LMM,\ i}$, $C_{MMM,\ i}$, $C_{HMM,\ i}$), and daily uptake rates of low and medium molecular mass compounds in intact leaves ($U_{LMM,\ i}$, $U_{MMM,\ i}$) (Fig. 6). All these variables were negatively related to Θ_{PM10} and $\Theta_{PM2.5}$ and clustered the samples of *D. draco*, while these traits partly separated *Citrus* × *aurantium* and *N. oleander* from the rest (Fig. 6).

4. Discussion

4.1. Leaf surface functional traits

Species co-existing in given climates share similar suites of foliage functional traits (Reich et al., 1999; Niinemets, 2001; Guerra and Scremin-Dias, 2017; Bu et al., 2019). Due to relatively high winter temperatures, the Mediterranean region has historically allowed cultivation of a wide range of temperate and tropical species, and using irrigation, even species from wet climates; the species have been introduced as food source as well as for purely ornamental purposes, leading to the increase of species diversity in cities up to the present day (Heywood, 2017). Many of the species analyzed in this work originate from or have been introduced in the Mediterranean area (POWO, 2023). Species such as *B. acerifolius*, *C. camphora*, *E. crista-galli*, *F. retusa* and *J. mimosifolia* are subtropical to tropical species introduced to the Mediterranean region for ornamental purposes (Heywood, 2017). *Magnolia grandiflora*, is sclerophyllous due to their leaf characteristics and can tolerate the climatic characteristics of the Mediterranean (Axelrod, 1975).

The leaves of studied species had widely differing leaf surface characteristics (Table S5). All the species had stomata on the lower surface, and four had amphistomatous leaves: *P. canariensis* (Xiong and Flexas, 2020), *E. camaldulensis* (Nogueira et al., 2018), *E. crista-galli* (Gratieri-Sossella, 2005) and *D. draco* (Klimko et al., 2018). Amphistomy is considered to be an ancient characteristic that is an evolutionary adaptation to hot and humid climate (Mott et al., 1982; Song et al., 2021).

In this study, the maximum $N_{s,\ l}$ found in *C. australis* samples (= 786 mm^{-2}, Table S5) was higher than that found previously in Mediterranean species (250 - 500 mm^{-2}, Bosabalidis and Kofidis, 2002; Yadav et al., 2004; Deng et al., 2017). *Phoenix canariensis* showed maximum average values for $N_{s,\ u}$ (= 421 mm^{-2}, Table S5), and our results are higher than data from Hodel et al. (2003), which found lower values (= 272 mm^{-2}). The large variation in the leaf area covered by stomatal

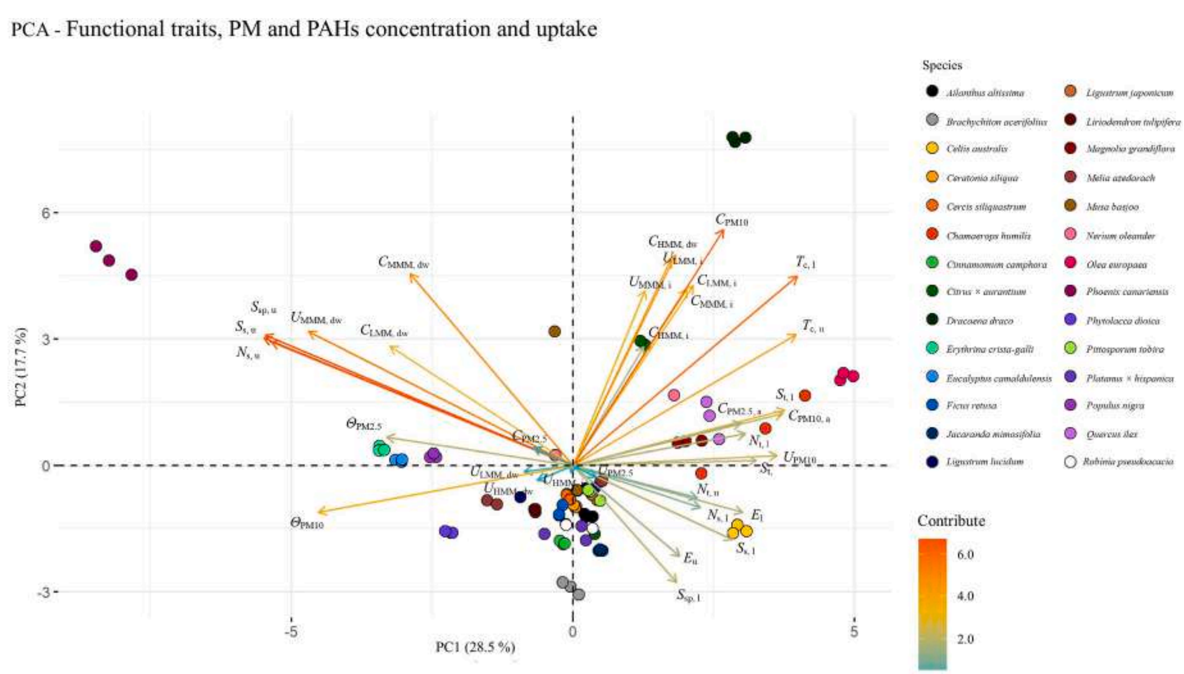

Fig. 6. Biplots of principal component analyses (PCA) biplot showing ordination of species in the PCA space determined by leaf surface functional traits, average PM and PAH concentrations (C) and daily uptake rates (U) and different contributions of traits to PCA axes. Plant samples and the included variables are expressed as symbols and vectors. The plots display the first (PC1) and second (PC2) principal components, variance explained by PC1 and PC2 and the variable contributions (as characterized by the length of the vectors) to the first two principal components. Functional traits symbols are defined in Table S2, other symbols are defined in Table S3.

pores and entire stomata uncovered in this study is highly relevant as these traits are useful to describe the area available for diffusion of pollutants into leaf interior (Prigioniero et al., 2022).

Quercus ilex with stellate trichomes had the greatest $S_{t,\ l}$ (Table S5; Fig. 2A) in agreement with previous studies (Deng et al., 2017; Prigioniero et al., 2022). *Chamaerops humilis* and *M. grandiflora* also had high values of $S_{t,\ l}$ despite having trichomes with less complex shapes, due to the high density of trichomes on the lower leaf surface (Table S5; Fig. 2D; Fig. 2E; Dransfield et al., 2008). *Platanus* × *hispanica*, on the contrary, although it had complex (dendritic) trichomes, had a low trichome density, resulting in low trichome surface area per leaf surface (Table S5; Fig. 2B; Carpenter et al., 2005). The average values of trichome traits in our study are higher than those found in another study on Mediterranean species (Yadav et al., 2004), indicating a presumable adaptation to an urban polluted environment (Pal et al., 2002; Balasooriya et al., 2009; Kardel et al., 2010; Kováts et al., 2021).

Cuticle thickness for both leaf sides ($T_{c,\ l}$ and $T_{c,\ u}$,Table S5) was similar to what found by Yadav et al. (2004) for other Mediterranean species, and within the range defined by Klimko et al. (2018) for *D. draco*, one of the species with highest values for $T_{c,\ l}$. As already noted in a previous work, infrared spectra displayed the distinctive features of the main cuticle components: cutin, waxes, polysaccharides and phenolic compounds (Fig. S1 in SM; da Luz, 2006; Heredia-Guerrero et al., 2014; Izzo et al., 2020; Prigioniero et al., 2022). Nanocosane, a component of the cuticle found in *O. europaea* leaves (Silverstein and Webster, 1998; da Luz, 2006), is present in all samples showing doublets at 1470-1460 cm^{-1} and 730-720 cm^{-1} (CH_2 aliphatic bending vibrations; Fig. S1 in SM). *Brachychiton acerifolius*, *C. australis*, *C. siliqua*, *J. mimosifolia*, *L. japonicum*, *M. grandiflora, M. azedarach, N. oleander,* and *Q. ilex* showed pronounced bifaciality, due to the difference in polysaccharides present in lower surface cuticle (Fig. S1 in SM). The spectral signature found by da Luz (2006) attributable to the presence of trichomes (ca. 1030 cm^{-1}) was found in all analyzed species with trichomes (Fig. S1 in SM). A band attributable to cutan was found in *C. humilis, E. crista-galli, M. basjoo,* and *P. canariensis*, explaining the lower value of the esterification index (Table S5; da Luz, 2006; Heredia-Guerrero et al., 2014). Trichomes presence could affect the esterification index assessment, and the presence of cutan instead cutin in the cuticle matrix, could affect the cuticle chemical properties, changing its hydrophobicity (Heredia-Guerrero et al., 2014; Prigioniero et al., 2022).

4.2. Pollutant concentrations and accumulation rates

The coefficient of variation of atmospheric particulate concentrations was considered low enough to use average concentrations to represent environmental conditions (Tables S3 and S4 in SM; Prigioniero et al., 2022). The atmospheric data collected indicate that there was no wind and rain action that could result in resuspension or leaching of PM from leaves (McPherson et al., 1998; Mo et al., 2015). In fact, in almost all species sampled, there was a strong increase in PM_{10} concentrated on leaves from August to September (Table S8). Exceptions were *C. siliqua*, *D. draco*, *E. camaldulensis*, *L. tulipifera*, *M. basjoo*, *P. canariensis* and *P. dioica* (Table S8). Looking at the characteristics of the leaves of these species, it jumps out that they are glabrous, and this could partially explain the lack of accumulation due to the absence of trichomes (Prigioniero et al., 2022). Looking at the data from the extractions on *D. draco* leaves, it is possible to observe that the coarse particulate matter extracted in water (and thus simply placed on the leaves) in September is approximately half of that extracted in August (Table S8), suggesting a resuspension that falls within the average data proposed in the literature (McPherson et al., 1998; Mo et al., 2015). Concentrations obtained from $PM_{2.5}$ extraction indicated that nine species out of 28 analyzed did not show an increase of pollutant in leaves during the study period (Table S8). The conditions of severe drought that lasted for thirty days may have contributed to this drop in particulate concentrations recorded in September (Lin et al., 2021). Unlike the PM_{10} case, the total amount of $PM_{2.5}$ extracted was more influenced by its fraction extracted in chloroform and therefore more intimately adhered to the cuticle (Table S8). This is also reflected in the hydrophobic fine particulate matter value ($\Theta_{PM2,5}$; 0.111–0. 959, Table S8) which is greater than hydrophobic PM_{10} value (Θ_{PM10}; 0.079–0. 794, Table S5). Leaf $PM_{2.5}$ concentrations ($C_{PM2.5}$) and uptake ($U_{PM2.5}$) were not well described by the principal component analysis, but PCA showed a negative correlation between $U_{PM2.5}$ and $\Theta_{PM2,5}$ (Fig. 5). The same relationship was clearly visible between U_{PM10} and Θ_{PM10} (Fig. 5) implying that the hydrophobicity of the leaf surface negatively influences the retention of particulate matter as driven by different functional traits (Dzierzanowski et al., 2011; Wang and Shi, 2021). A positive correlation was found between atmospheric concentrations of coarse particulate matter ($C_{PM10,\ a}$) and uptake of PM_{10} (Fig. 5). The highest PM_{10} concentrations obtained in the first sampling of this study are comparable with those found in urban environments by Sæbø et al. (2012) and Song et al. (2015), with the exception of *D. draco*, from whose leaves twice as much was extracted as in previous works (Table S8). The same applies to *O. europaea* and *C. humilis*, from whose leaves sampled in September, twice as much coarse PM was extracted as reported in the aforementioned papers (Table S8). Song et al. (2015) found lower amounts of $PM_{2.5}$ than the analyses in this paper (Table S9), but the proportions of fine and coarse particulate matter on plant matrices remain comparable (Popek et al., 2013; Song et al., 2015). When comparing the results of the present study with those found in similar works, it must be considered that there are differences regarding the plant species analyzed and the urban environmental context that determines the pollution to which the plants are exposed. So the comparison itself must be done with due care and it is not surprising if differences are highlighted.

The amounts of PAH found in intact leaves represent the sum of pollutants on the leaf surface (eventually bound to the cuticle) with those translocated into the subcuticular tissues (Prigioniero et al., 2022). Data on PAH in intact leaves found in *D. draco* (LMM and MMM), *L. lucidum* (MMM) and *E. crista-galli* (HMM) were consistent with the findings of Fasani et al. (2016) who related the absence of trichomes to higher accumulation of three- and four-ring slowly diffusing PAH. Cutin is the main contributor in PAH accumulation, limiting their movement to the sub-epidermal tissues (Shechter and Chefetz, 2008; Chen and Schnoor, 2009; Li et al., 2010; Mętrak et al., 2016). This was consistent with our data about *P. canariensis* LMM and MMM uptake in dewaxed leaves, due the presence of cutan as major component of cuticle (Shechter and Chefetz, 2008).

4.3. Clustering of species according to functional traits, PM and PAH concentrations and uptake

The results emerged from this work highlighted the existence of positive correlations between functional traits related to stomata on the upper leaf surface ($S_{s,\ u}$, $S_{sp,\ u}$, $N_{s,\ u}$), the concentration and uptakes of MMM PAH and the concentration of LMM PAH in dewaxed leaves (Fig. 5). These variables grouped *P. canariensis*, *E. camaldulensis*, *E. crista-galli* and *P. nigra* finding corroboration with the assertions and investigation of other authors (Gratieri-Sossella, 2005; Nogueira et al., 2018; Xiong and Flexas, 2020). This correlation, could lead to misinterpretation, avoidable considering the Mediterranean environment climatic characteristics, well expressed in the summer month in which sampling was carried out, during which there was no atmospheric precipitation. Stomatal uptakes depends on water availability that could induce or avoid stomatal opening (Fowler et al., 2009; Niinemets et al., 2014). Taking this into account, the results obtained are not comparable to other work that correlates these variables on the basis of stomatal conductivity given by the opening of stomata (Kováts et al., 2021), since in an arid summer month it is unlikely that plants, especially sclerophyllous, would have opened their stomata for long enough to allow the passage and accumulation of PAH in subcuticular tissues (Lange et al., 1982; Reichstein et al., 2002; Niinemets and Keenan, 2014). The reasons for this correlation can be searched by looking at the presence of a negative correlation existing between the above group of variables and cuticle thickness (Fig. 5). The traits of cuticular thicknesses are also positively correlated with the concentrations and uptakes of PAH in intact leaves (Fig. 5). These relationships were assessed by Shahid et al. (2016) who found that stomatal areas present a breach in the impenetrability of the cuticle due to a thinning of cuticle at the area occupied by stomata that favors the entry of pollutants into tissues located below it. Relationships between cuticle thickness, concentrations, and pollutant uptake are corroborated by the fact that there are pores within plant cuticles these are fewer in thicker cuticles for which pollutant infiltration is hindered (Schönherr, 2006; Tredenick et al., 2017). *Citrus* × *aurantium* showed great attitude to concentrate and accumulate LMM and MMM hydrocarbons, in this work and in others (Fasani et al., 2016). The negative correlation between PAH uptake in dewaxed leaves and esterification indices, found in previous work was confirmed (Fig. 5), reinforcing the assertion that cutin is a very effective barrier to prevent pollutants translocation (Prigioniero et al., 2022). The prevalence of cutan instead of cutin in *P. canariensis* would result in the lowest E_u and E_u allowing pollutant translocation (Chen and Schnoor, 2009; Li et al., 2010; Mętrak et al., 2016). Θ_{PM10} and $\Theta_{PM2.5}$ scaled negatively with cuticle thickness, PAH concentration and uptake in intact leaves and esterification index (Fig. 5) This hydrophobicity most affected the concentration over time of fine particulate matter, and the $U_{LMM,\ dw}$, and $U_{HMM,\ dw}$, characterizing and justifying the location of *E. crista-galli*, *P. nigra*, *E. camaldulensis*, *P. dioica* and *M. azedarach* samples (Fig. 5). The dependence of the cuticle chemical composition in the hydrocarbons penetration into the leaf tissues is supported by these results reflected in the literature (Domínguez et al., 2015).

C_{PM10} found in our investigation are similar as observed previously in leaves of Mediterranean species (Esposito et al., 2020; Sgrigna et al., 2015), and correlated positively with cuticle thickness and concentrations of PAH in the intact leaf in line with other studies looking at particulate matter as a carrier for the transport of hydrocarbons (Yang et al., 2021). U_{PM10} was positively correlated with trichome traits ($N_{t,\ l}$, $S_{t,\ l}$, $N_{t,\ u}$ and $S_{t,\ u}$) (Fig. 5). *Chamaerops humilis, Q. ilex, O. europaea* and *M. grandiflora* are grouped positioned in that area of the graph by the presence of trichomes on their surfaces, and the uptake of coarse particulate matter (Fig. 5). High trichome number and surface area, characterized these species and justified their ability to concentrate PM_{10} (Fig. 5). The concentrations of particulate matter ($C_{PM10,\ a}$ and $C_{PM2.5,\ a}$) in the air helped to group and discriminate these four species, also due to a positive correlation with the uptake of PM_{10} (Fig. 5). The ability of *Q. ilex* to sequester PAH has been assessed by other authors (De Nicola et al., 2005; Orecchio, 2007), but, we demonstrated that it is the trichome surface that determines its capacity to sequester particulate matter. Studies suggested that high trichome density allows pollutants to accumulate on trichome layers preventing the contact and penetration through the cuticle (Jouraeva et al., 2003; Li et al., 2010; Domínguez et al., 2015). In line with these findings, negative correlations between MMM PAH uptake in dewaxed leaves were observed with trichome traits across species (Fig. 5). One limit of this work was the lack of data about PAH concentration in atmosphere, this did not allow to assess the correlation between $PM_{2.5}$ and PAH air concentration observed in other studies (Liu et al., 2017). Many works approached at functional traits considered as leaf shape (Esposito et al., 2020) or microstructures of the leaves (Zhang et al., 2018; Baraldi et al., 2019; Li et al., 2010), but the role of trichome-driven increase of leaf surfaces in particulate matter absorption and retention were not deeply investigated.

In this work, the detailed characterization of leaf surface functional traits adds to and complements the knowledge of functional traits useful for air phytoremediation (Grote et al., 2016; Kattge et al., 2020). New and more detailed information were obtained on the functional leaf morphologies of tree species. Given the peculiarity of the urban Mediterranean environment and those of the leaf traits adapted in it, we consider the impact of these new data. The leaf economic spectrum of Wright et al. (2004) considers as key leaf traits, Leaf mass per area (LMA), Photosynthetic assimilation rates, Leaf nitrogen and phosphorus, Dark respiration rate and Leaf lifespan, however, especially considering the evaluation and application of NBS, these traits may not be sufficient. We have brought out a number of highly relevant traits that are not included in the leaf economic spectrum and that we consider important to study when evaluating nature-based solutions. The characterisation of leaf functional traits of 28 tree species allowed us to obtain valuable data to suggest new and implement existing patterns of pollutant retention and pollutant translocation prevention or promotion into the leaf epidermis and non-hydrophobic regions. The difference in leaf surface functional traits related to trichomes, stomata and cuticle justify part of the different plant performance in air phytoremediation. In this study, albeit partially, we defined new data on such a complex mechanism as the dry deposition of pollutants in relation to functional traits, rather than in relation to the specific identity of the plant organism. These new insights will allow the development of studies in different environmental contexts and with different species, the results of which will be comparable precisely on the basis of the redundancy of functional traits. Trichomes increase the leaf surface area and complexity, and resulted important in the study of particulate matter fluxes from atmosphere to plant canopies. Cuticle physical and chemical features regulate PAH accumulation by leaves and their translocation into the subcuticular tissue. In this work, only leaf surface functional traits were considered, excluding economic leaf spectrum traits (Wright et al., 2004). However, a positive correlation between leaf dry mass and cuticle thickness has been demonstrated (Niinemets, 2002), and this opens up the possibility and need for further study of functional traits in order to better clarify their role in the relationship plants have with the environment. More efforts in this direction will allow us also to fully understand the role of each leaf traits in air phytoremediation, completing the knowledge useful to select and even improve high performance plant species able to be efficient NBS.

CRediT authorship contribution statement

Antonello Prigioniero: Investigation, Validation, Conceptualization, and, Writing – original draft. **Alessia Postiglione:** Investigation, Validation, Conceptualization, and, Writing – original draft. **Daniela Zuzolo:** Conceptualization, Visualization, Data curation, and, Formal analysis, Writing – review & editing. **Ülo Niinemets:** Validation, Supervision, and, Writing – review & editing. **Maria Tartaglia:** Data curation. **Pierpaolo Scarano:** Data curation. **Mariano Mercurio:** Investigation, Visualization. **Chiara Germinario:** Investigation, Visualization. **Francesco Izzo:** Investigation, Visualization. **Marco Trifuoggi:** Investigation. **Maria Toscanesi:** Investigation. **Rosaria Sciarrillo:** Conceptualization, and, Supervision. **Carmine Guarino:** Conceptualization, and Supervision.

Declaration of competing interest

The authors declare that they have no competing financial interests or personal relationships that could have appeared to influence the work reported in this paper.

Data availability

Data will be made available on request.

Appendix A. Supplementary data

Supplementary data to this article can be found online at https://doi.org/10.1016/j.jclepro.2023.138158.

References

Anderson, J.O., Thundiyil, J.G., Stolbach, A., 2012. Clearing the air: a review of the effects of particulate matter air pollution on human health. J. Med. Toxicol. 8 (2), 166–175. https://doi.org/10.1007/s13181-011-0203-1.

Axelrod, D.I., 1975. Evolution and biogeography of madrean-tethyan sclerophyll vegetation. Ann. Mo. Bot. Gard. 62, 280–334. https://doi.org/10.2307/2395199.

Balasooriya, B.L.W.K., Samson, R., Mbikwa, F., Vitharana, U.W.A., Boeckx, P., Van Meirvenne, M., 2009. Biomonitoring of urban habitat quality by anatomical and chemical leaf characteristics. Environ. Exp. Bot. 65 (2–3), 386–394. https://doi.org/10.1016/j.envexpbot.2008.11.009.

Baraldi, R., Chieco, C., Neri, L., Facini, O., Rapparini, F., Morrone, L., Rotondi, A., Carriero, G., 2019. An integrated study on air mitigation potential of urban vegetation: from a multi-trait approach to modeling. Urban For. Urban Green. 41, 127–138. https://doi.org/10.1016/j.ufug.2019.03.020.

Blanusa, T., Fantozzi, F., Monaci, F., Bargagli, R., 2015. Leaf trapping and retention of particles by holm oak and other common tree species in Mediterranean urban environments. Urban For. Urban Green. 14, 4. https://doi.org/10.1016/j.ufug.2015.10.004.

Bosabalidis, A.M., Kofidis, G., 2002. Comparative effects of drought stress on leaf anatomy of two olive cultivars. Plant Sci. 163, 375–379. https://doi.org/10.1016/S0168-9452(02)00135-8.

Brazkova, M., Krastanov, A.I., 2013. Polycyclic Aromatic Hydrocarbons: Sources, Effects and Biodegradation. International Scientific Conference of University of Ruse At: Razgrad, Bulgaria, p. 52.

Brook, R.D., Rajagopalan, S., Pope 3rd, C.A., Brook, J.R., Bhatnagar, A., Diez-Roux, A.V., Holguin, F., Hong, Y., Luepker, R.V., Mittleman, M.A., et al., 2010. Particulate matter air pollution and cardiovascular disease: an update to the scientific statement from the American Heart Association. Circulation. American Heart Association Council on Epidemiology and Prevention, Council on the Kidney in Cardiovascular Disease, and Council on Nutrition, Physical Activity and Metabolism 121 (21), 2331–2378. https://doi.org/10.1161/CIR.0b013e3181dbece1.

Bu, W., Huang, J., Xu, H., Zang, R., Ding, Y., Li, Y., Lin, M., Wang, J., Zhang, C., 2019. Plant functional traits are the mediators in regulating effects of abiotic site conditions on aboveground carbon stock-evidence from a 30 ha tropical forest plot. Front. Plant Sci. 9, 1958. https://doi.org/10.3389/fpls.2018.01958.

Burkhardt, J., 2010. Hygroscopic particles on leaves: nutrients or desiccants? Ecol. Monogr. 80, 369–399. https://doi.org/10.1890/09-1988.1.

Cariñanos, P., Casares-Porcel, M., Díaz de la Guardia, C., Aira, M.J., Belmonte, J., Boi, M., Elvira-Rendueles, B., De Linares, C., Fernández-Rodriguez, S., Maya-Manzano, J.M., et al., 2017. Assessing allergenicity in urban parks: a nature-based solution to reduce the impact on public health. Environ. Res. 155, 219–227. https://doi.org/10.1016/j.envres.2017.02.015.

Carpenter, R.J., Hill, R.S., Jordan, G.J., 2005. Leaf cuticular morphology links platanaceae and proteaceae. Int. J. Plant Sci. 166 (5), 843–855. https://doi.org/10.1086/431806.

Chen, B., Schnoor, J.L., 2009. Role of suberin, suberan, and hemicellulose in phenanthrene sorption by root tissue fractions of switchgrass (*Panicum virgatum*) seedlings. Environ. Sci. Technol. 43, 4130–4136. https://doi.org/10.1021/es803510u.

Chen, Q., Wang, F., Yang, H., Wang, X., Zhang, A., Ling, X., Li, L., Zou, P., Sun, L., Huang, L., et al., 2021. Exposure to fine particulate matter-bound polycyclic aromatic hydrocarbons, male semen quality, and reproductive hormones: the MARCHS study. Environ. Pollut. 280, 116883 https://doi.org/10.1016/j.envpol.2021.116883.

da Luz, B.R., 2006. Attenuated total reflectance spectroscopy of plant leaves: a tool for ecological and botanical studies. New Phytol. 172, 305–318.

De Nicola, F., Maisto, G., Prati, M.V., Alfani, A., 2005. Temporal variations in PAH concentrations in *Quercus ilex* L. (holm oak) leaves in an urban area. Chemosphere 61 (3), 432–440. https://doi.org/10.1016/j.chemosphere.2005.01.082.

Deng, M., Jiang, X.L., Song, Y.G., Coombes, A., Yang, X.R., Xiong, Y.S., Li, Q.S., 2017. Leaf epidermal features of *Quercus* Group *ilex* (Fagaceae) and their application to species identification. Rev. Palaeobot. Palynol. 237, 10–36. https://doi.org/10.1016/j.revpalbo.2016.11.006.

Domínguez, E., Heredia-Guerrero, J.A., Heredia, A., 2015. Plant cutin genesis: unanswered questions. Trends Plant Sci. 20, 551–558. https://doi.org/10.1016/j.tplants.2015.05.009.

Dransfield, J., Uhl, N.W., Asmussen, C.B., Baker, W.J., Harley, M.M., Lewis, C.E., 2008. Genera Palmarum the Evolution and Classification of Palms, 978-1-84246-182-2.

Dzierzanowski, K., Popek, R., Gawrońska, H., Saebø, A., Gawroński, S.W., 2011. Deposition of particulate matter of different size fractions on leaf surfaces and in waxes of urban forest species. Int. J. Phytoremediation 13, 1037–1046. https://doi.org/10.1080/15226514.2011.552929.

Esposito, F., Memoli, V., Panico, S.C., Di Natale, G., Trifuoggi, M., Giarra, A., Maisto, G., 2020. Leaf traits of *Quercus ilex* L. affect particulate matter accumulation. Urban For. Urban Green. 54, 126780 https://doi.org/10.1016/j.ufug.2020.126780.

Fasani, D., Fermo, P., Barroso, P.J., Martín, J., Santos, J.L., Aparicio, I., Alonso, E., 2016. Analytical method for biomonitoring of pah using leaves of bitter orange trees (*Citrus aurantium*): a case study in South Spain. Water, Air, Soil Pollut. 227 https://doi.org/10.1007/s11270-016-3056-z.

Fellet, G., Pošćić, F., Licen, S., Marchiol, L., Musetti, R., Tolloi, A., Barbieri, P., Zerbi, G., 2016. PAHs accumulation on leaves of six evergreen urban shrubs: a field experiment. Atmos. Pollut. Res. 7, 915–924. https://doi.org/10.1016/j.apr.2016.05.007.

Forbes, L.J., Kapetanakis, V., Rudnicka, A.R., Cook, D.G., Bush, T., Stedman, J.R., Whincup, P.H., Strachan, D.P., Anderson, H.R., 2009. Chronic exposure to outdoor air pollution and lung function in adults. Thorax 64 (8), 657–663. https://doi.org/10.1136/thx.2008.109389.

Fortelli, A., Scafetta, N., Mazzarella, A., 2016. Influence of synoptic and local atmospheric patterns on PM10 air pollution levels: a model application to Naples (Italy). Atmos. Environ. 143, 218–228. https://doi.org/10.1016/j.atmosenv.2016.08.050.

Fowler, D., Pilegaard, K., Sutton, M.A., Ambus, P., Raivonen, M., Duyzer, J., Simpson, D., Fagerli, H., Fuzzi, S., Schjoerring, J.K., et al., 2009. Atmospheric composition change: ecosystems - atmosphere interactions. Atmos. Environ. 43, 5193–5267.

Gaglio, M., Pace, R., Muresan, A.N., Grote, R., Castaldelli, G., Calfapietra, C., Fano, E.A., 2022. Species-specific efficiency in $PM_{2.5}$ removal by urban trees: from leaf measurements to improved modeling estimates. Sci. Total Environ. 844, 157131 https://doi.org/10.1016/j.scitotenv.2022.157131.

Gómez-Moreno, F.J., Artíñano, B., Ramiro, E.D., Barreiro, M., Núñez, L., Coz, E., Dimitroulopoulou, C., Vardoulakis, S., Yagüe, C., Maqueda, G., Sastre, M., Román-Cascón, C., Santamaría, J.M., Borge, R., 2019. Urban vegetation and particle air pollution: experimental campaigns in a traffic hotspot. Environ. Pollut. 247, 195–205. https://doi.org/10.1016/j.envpol.2019.01.016.

Gratieri-Sossella, A., 2005. Potencialidade ornamental e paisagística, caracterização morfo-anatômica e propagação de *Erythrina cristagalli* L. *Dissertação de Mestrado, Programa de Pósgraduação em Agronomia*. Universidade de Passo Fundo.

Grote, R., Samson, R., Alonso, R., Amorim, J.A., Cariñanos, P., Churkina, G., Fares, S., Le Thiec, D., Niinemets, Ü., Mikkelsen, T.N., et al., 2016. Functional traits of urban trees: air pollution mitigation potential. Front. Ecol. Environ. 14 (10), 543–550. https://doi.org/10.1002/fee.1426.

Guerra, A., Scremin-Dias, E., 2017. Leaf traits, sclerophylly and growth habits in plant species of a semiarid environment. Braz. J. Bot. 41, 1. https://doi.org/10.1007/s40415-017-0416-x.

Hamanaka, R.B., Mutlu, G.M., 2018. Particulate matter air pollution: effects on the cardiovascular system. Front. Endocrinol. 9, 680. https://doi.org/10.3389/fendo.2018.00680.

Heredia-Guerrero, J.A., Benítez, J.J., Domínguez, E., Bayer, I.S., Cingolani, R., Athanassiou, A., Heredia, A., 2014. Infrared and Raman spectroscopic features of plant cuticles: a review. Front. Plant Sci. 5 https://doi.org/10.3389/fpls.2014.00305.

Heywood, V.H., 2017. The nature and composition of urban plant diversity in the Mediterranean. Fl. Medit 27, 195–220. https://doi.org/10.7320/FlMedit27.195.

Hodel, D.R., Pittenger, D.R., Downer, A.J., Richie, W.E., 2003. Effect of leaf removal and tie up on juvenile, transplanted canary island date palms (*Phoenix canariensis*) and queen palms (*Syagrus romanzoffiana*). Palms 47, 4.

Izzo, F., Germinario, C., Grifa, C., Langella, A., Mercurio, M., 2020. External reflectance FTIR dataset (4000–400 cm^{-1}) for the identification of relevant mineralogical phases forming Cultural Heritage material. Infrared Phys. Technol. 106, 103266 https://doi.org/10.1016/j.infrared.2020.103266.

Janhall, S., 2015. Review on urban vegetation and particle air pollution-Deposition and dispersion. Atmos. Environ. 105, 130e137. https://doi.org/10.1016/j.atmosenv.2015.01.052.

Jouraeva, V.A., Johnson, D.L., Hassett, J.P., Nowak, D.J., 2003. Differences in accumulation of PAHs and metals on leaves of *Tilia* × *euchlora* and *Pyrus calleryana*. ACS, Div. Environ. Chem. - Prepr. Ext. Abstr. 43, 52–56.

Kampa, M., Castanas, E., 2008. Human health effects of air pollution. Environ. Pollut. 151 (2), 362–367. https://doi.org/10.1016/j.envpol.2007.06.012.

Kardel, F., Wuyts, K., Babanezhad, M., Vitharana, U.W.A., Wuytack, T., Potters, G., Samson, R., 2010. Assessing urban habitat quality based on specific leaf area and stomatal characteristics of *Plantago lanceolata* L. Environ. Pollut. 158, 788–794. https://doi.org/10.1016/j.envpol.2009.10.006.

Kattge, J., Bönisch, G., Díaz, S., et al., 2020. TRY plant trait database – enhanced coverage and open access. Global Change Biol. 26, 119–188. https://doi.org/10.1111/gcb.14904.

Klimko, M., Nowińska, R., Wilkin, P., et al., 2018. Comparative leaf micromorphology and anatomy of the dragon tree group of *Dracaena* (Asparagaceae) and their taxonomic implications. Plant Systemat. Evol. 304, 1041–1055. https://doi.org/10.1007/s00606-018-1530-3.

Kottek, M., Grieser, J., Beck, C., Rudolf, B., Rubel, F., 2006. World map of the Köppen-Geiger climate classification updated. Meteorol. Z. 15, 259–263. https://doi.org/10.1127/0941-2948/2006/0130.

Kováts, N., Hubai, K., Diósi, D., Sainnokhoi, T.A., Hoffer, A., Tóth, A., Teke, G., 2021. Sensitivity of typical European roadside plants to atmospheric particulate matter. Ecol. Indicat. 124, 107428 https://doi.org/10.1016/j.ecolind.2021.107428.

La Riva, E.G., Villar, R., Pérez-Ramos, I.M., Quero, J.L., Matías, L., Poorter, L., Marañón, T., 2018. Relationships between leaf mass per area and nutrient concentrations in 98 Mediterranean woody species are determined by phylogeny, habitat and leaf habit. Trees (Berl.) 32, 497–510. https://doi.org/10.1007/s00468-017-1646-z.

Landrigan, P.J., 2017. Air pollution and health. Lancet Public Health 2 (1), e4–e5. https://doi.org/10.1016/S2468-2667(16)30023-8.

Lange, O.L., Tenhunen, J.D., Brau, M., 1982. Midday stomatal closure in Mediterranean type sclerophylls under simulated habitat conditions in an environmental chamber. I. Comparison of the behaviour of various European Mediterranean species. Flora 172, 563–579.

Li, Q., Li, Y., Zhu, L., Xing, B., Chen, B., 2017. Dependence of plant uptake and diffusion of polycyclic aromatic hydrocarbons on the leaf surface morphology and micro-structures of cuticular waxes. Sci. Rep. 7, 46235 https://doi.org/10.1038/srep46235.

Li, Y., Chen, B., Zhu, L., 2010. Single-solute and bi-solute sorption of phenanthrene and pyrene onto pine needle cuticular fractions. Environ. Pollut. 158, 2478–2484. https://doi.org/10.1016/j.envpol.2010.03.021.

Lin, X., Shu, D., Zhang, J., Chen, J., Zhou, Y., Chen, C., 2021. Dynamics of particle retention and physiology in *Euonymus japonicus* Thunb. var. *aurea-marginatus* Hort. with severe exhaust exposure under continuous drought. Environ. Pollut. 285, 117194 https://doi.org/10.1016/j.envpol.2021.117194.

Liu, D., Lin, T., Syed, J.H., Cheng, Z., Xu, Y., Li, K., Zhang, G., Li, J., 2017. Concentration, source identification, and exposure risk assessment of PM2.5-bound parent PAHs and nitro-PAHs in atmosphere from typical Chinese cities. Sci. Rep. 7, 1–12. https://doi.org/10.1038/s41598-017-10623-4.

Livesley, S.J., McPherson, G.M., Calfapietra, C., 2016. The urban forest and ecosystem services: impacts on urban water, heat, and pollution cycles at the tree, street, and city scale. J. Environ. Qual. 45 (1), 119–124. https://doi.org/10.2134/jeq2015.11.0567.

Losacco, C., Perillo, A., 2018. Particulate matter air pollution and respiratory impact on humans and animals. Environ. Sci. Pollut. Res. Int. 25 (34), 33901–33910. https://doi.org/10.1007/s11356-018-3344-9.

Łukowski, A., Popek, R., Karolewski, P., 2020. Particulate matter on foliage of *Betula pendula, Quercus robur*, and *Tilia cordata*: deposition and ecophysiology. Environ. Sci. Pollut. Res. 27, 10296–10307. https://doi.org/10.1007/s11356-020-07672-0.

Marando, F., Salvatori, E., Fusaro, L., Manes, F., 2016. Removal of PM_{10} by forests as a nature-based solution for air quality improvement in the metropolitan city of rome. Forests 7 (7), 150. https://doi.org/10.3390/f7070150.

McPherson, E.G., Scott, K.I., Simpson, J.R., 1998. Estimating cost effectiveness of residential yard trees for improving air quality in Sacramento, California, using existing models. Atmos. Environ. 32, 75–84. https://doi.org/10.1016/S1352-2310(97)00180-5.

Mętrak, M., Aneta, E., Wiłkomirski, B., Staszewski, T., Suska-Malawska, M., 2016. Interspecific differences in foliar 1 PAHs load between Scots pine, birch, and wild rosemary from three polish peat bogs. Environ. Monit. Assess. 188, 1–13. https://doi.org/10.1007/s10661-016-5465-2.

Mihankhah, T., Saeedi, M., Karbassi, A., 2020. Contamination and cancer risk assessment of polycyclic aromatic hydrocarbons (PAHs) in urban dust from different land-uses in the most populated city of Iran. Ecotoxicol. Environ. Saf. 187, 109838 https://doi.org/10.1016/j.ecoenv.2019.109838.

Mo, L., Ma, Z., Xu, Y., Sun, F., Lun, X., Liu, X., Chen, J., Yu, X., 2015. Assessing the capacity of plant species to accumulate particulate matter in Beijing, China. PLoS One 10, 1–18. https://doi.org/10.1371/journal.pone.0140664.

Mott, K.A., Gibson, A.C., O'Leary, J.W., 1982. The adaptive significance of amphistomatic leaves. Plant Cell Environ. 5, 455–460. https://doi.org/10.1111/1365-3040.ep11611750.

Mukherjee, A., Agrawal, M., 2018. Use of GLM approach to assess the responses of tropical trees to urban air pollution in relation to leaf functional traits and tree characteristics. Ecotoxicol. Environ. Saf. 152, 42–54. https://doi.org/10.1016/j.ecoenv.2018.01.038.

Niinemets, Ü., Fares, S., Harley, P., Jardine, K.J., 2014. Bidirectional exchange of biogenic volatiles with vegetation: emission sources, reactions, breakdown and deposition. Plant Cell Environ. 37, 1790–1809. https://doi.org/10.1111/pce.12322.

Niinemets, Ü., Keenan, T.F., 2014. Photosynthetic responses to stress in Mediterranean evergreens: mechanisms and models. Environ. Exp. Bot. 103, 24–41.

Niinemets, Ü., 2001. Global-scale climatic controls of leaf dry mass per area, density, and thickness in trees and shrubs. Ecology 82 (2), 453–469. https://doi.org/10.2307/2679872.

Niinemets, Ü., 2002. Research review. Components of leaf dry mass per area – thickness and density – alter leaf photosynthetic capacity in reverse directions in woody plants. New Phytol. 144, 35–47. https://doi.org/10.1046/j.1469-8137.1999.00466.x.

Niinemets, Ü., 2010. Responses of forest trees to single and multiple environmental stresses from seedlings to mature plants: past stress history, stress interactions, tolerance and acclimation. For. Ecol. Manag. 260 (10), 1623–1639. https://doi.org/10.1016/j.foreco.2010.07.054.

Nogueira, R., Rodrigueers, T., Camargo Campoe, O., Nouvellon, Y., Laclau, J.P., Le Maire, G., Stape, J.L., 2018. Differences in leaf traits among sixteen *Eucalyptus* genotypes suggest contrasting strategies to cope with climatic conditions. Abstracts book. CIRAD, IUFRO, MUSE 157–158.

Nowak, D.J., Hirabayashi, S., Bodine, A., Greenfield, E., 2014. Tree and forest effects on air quality and human health in the United States. Environ. Pollut. 193, 119–129. https://doi.org/10.1016/j.envpol.2014.05.028.

Orecchio, S., 2007. PAHs associated with the leaves of *Quercus ilex* L.: extraction, GC–MS analysis, distribution and sources: assessment of air quality in the Palermo (Italy) area. Atmos. Environ. 41 (38), 8669–8680. https://doi.org/10.1016/j.atmosenv.2007.07.027.

Pal, A., Kulshreshtha, K., Ahmad, K.J., Behl, H.M., 2002. Do leaf surface characters play a role in plant resistance to auto-exhaust pollution? Flora 197, 47–55. https://doi.org/10.1078/0367-2530-00014.

Popek, R., Gawrońska, H., Wrochna, M., Gawroński, S.W., Sæbø, A., 2013. Particulate matter on foliage of 13 woody species: deposition on surfaces and phytostabilisation in Waxes–a 3-Year study. Int. J. Phytoremediation 15, 245–256. https://doi.org/10.1080/15226514.2012.694498.

POWO, 2023. Plants of the world online. Facilitated by the royal botanic gardens. Kew. Published on the Internet. http://www.plantsoftheworldonline.org/. (Accessed 1 March 2023).

Prigioniero, A., Zuzolo, D., Niinemets, Ü., Postiglione, A., Mercurio, M., Izzo, F., Trifuoggi, M., Toscanesi, M., Scarano, P., Tartaglia, M., et al., 2022. Particulate matter and polycyclic aromatic hydrocarbon uptake in relation to leaf surface functional traits in Mediterranean evergreens: potentials for air phytoremediation. J. Hazard Mater. 435, 129029 https://doi.org/10.1016/j.jhazmat.2022.129029.

R Core Team, 2015. A Language and Environment for Statistical Computing. R Foundation for Statistical Computing, Vienna, Austria. -900051-07-0, URL, R.

Reich, P.B., Ellsworth, D.S., Walters, M.B., Vose, J.M., Gresham, C., Volin, J.C., Bowman, W.D., 1999. Generality of leaf trait relationships: a test across six biomes. Ecology 80, 1955–1969.

Reichstein, M., Tenhunen, J.D., Roupsard, O., Ourcival, J.-M., Rambal, S., Miglietta, F., Peressotti, A., Pecchiari, M., Tirone, G., Valentini, R., 2002. Severe drought effects on ecosystem CO_2 and H_2O fluxes at three Mediterranean evergreen sites: revision of current hypothesis? Global Change Biol. 8, 1–19.

Sæbø, A., Popek, R., Nawrot, B., Hanslin, H., Gawronska, H., Gawronski, S., 2012. Plant species differences in particulate matter accumulation on leaf surfaces. Sci. Total Environ. 427, 347–354. https://doi.org/10.1016/j.scitotenv.2012.03.084. **–428**.

Samson, R., Grote, R., Calfapietra, C., Cariñanos, P., Fares, S., Paoletti, E., Tiwary, A., 2017. Urban trees and their relation to air pollution. In: The Urban Forest. *Future City* Springer, Cham. https://doi.org/10.1007/978-3-319-50280-9_3.

Schönherr, J., 2006. Characterization of aqueous pores in plant cuticles and permeation of ionic solutes. J. Exp. Bot. 57, 2471–2491. https://doi.org/10.1093/jxb/erj217.

Sgrigna, G., Sæbø, A., Gawronski, S., Popek, R., Calfapietra, C., 2015. Particulate Matter deposition on *Quercus ilex* leaves in an industrial city of central Italy. Environ. Pollut. 197, 187–194. https://doi.org/10.1016/j.envpol.2014.11.030.

Shahid, M., Dumat, C., Khalid, S., Schreck, Xiong, T., Niazi, N.K., 2016. Foliar heavy metal uptake, toxicity and detoxification in plants: a comparison of foliar and root metal uptake. J. Hazard Mater. 325, 36–58.

Shechter, M., Chefetz, B., 2008. Insights into the sorption properties of cutin and cutan biopolymers. Environ. Sci. Technol. 42, 1165–1171. https://doi.org/10.1021/es702205u.

Silverstein, R.M., Webster, F.X., 1998. Spectrometric Identification of Organic Compounds, sixth ed. John Wiley & Sons, New York, NY, USA, pp. 71–143.

Song, A., Liu, J., Liang, S.-G., Do, T.V., Nguyen, H.B., Deng, W.-Y.-B., Jia, L.-B., Del Rio, C., Srivastava, G., Feng, Z., et al., 2021. Leaf fossils of *Sabalites* (Arecaceae) from the Oligocene of northern Vietnam and their paleoclimatic implications. Plant Diversity 44, 406–416. https://doi.org/10.1016/j.pld.2021.08.003.

Song, Y., Maher, B.A., Li, F., Wang, X., Sun, X., Zhang, H., 2015. Particulate matter deposited on leaf of five evergreen species in Beijing, China: source identification and size distribution. Atmos. Environ. 105, 53–60. https://doi.org/10.1016/j.atmosenv.2015.01.032.

Terzaghi, E., Wild, E., Zacchello, G., Cerabolini, B.E.L., Jones, K.C., Di Guardo, A., 2013. Forest Filter Effect: role of leaves in capturing/releasing air particulate matter and its associated PAHs. Atmos. Environ. 74, 378–384. https://doi.org/10.1016/j.atmosenv.2013.04.013.

Thangjai, W., Niwitpong, S.A., Niwitpong, S., 2021. A bayesian approach for estimation of coefficients of variation of normal distributions. Sains Malays. 50, 261–278. https://doi.org/10.17576/jsm-2021-5001-25.

Tredenick, E.C., Farrell, T.W., Forster, W.A., Psaltis, S.T.P., 2017. Nonlinear porous diffusion modeling of hydrophilic Ionic agrochemicals in astomatous plant cuticle aqueous pores: a mechanistic approach. Front. Plant Sci. 8, 746. https://doi.org/10.3389/fpls.2017.00746.

Wang, H., Shi, H., 2021. Particle retention capacity, efficiency, and mechanism of selected plant species: implications for urban planting for improving urban air quality. Plants 10, 2109. https://doi.org/10.3390/plants10102109.

Wickham, H., 2016. ggplot2: Elegant Graphics for Data Analysis. Springer-Verlag, New York, ISBN 978-3-319-24277-4. https://ggplot2.tidyverse.org.

Wright, I.J., Reich, P.B., Westoby, M., Ackerly, D.D., Baruch, Z., Bongers, F., Cavender-Bares, J., Chapin, T., Cornelissen, J.H.C., Diemer, M., et al., 2004. The world-wide leaf economics spectrum. Nature 428, 821–827.

Xiong, D., Flexas, J., 2020. From one side to two sides: the effects of stomatal distribution on photosynthesis. New Phytol. 228, 1754–1766. https://doi.org/10.1111/nph.16801.

Yadav, R.K.P., Bosabalidis, A.M., Vokou, D., 2004. Leaf structural features of Mediterranean perennial species: plasticity and life form specificity. J. Biol. Res. 2, 21–34.

Yang, L., Zhang, H., Zhang, X., Xing, W., Wang, Y., Bai, P., Zhang, L., Hayakawa, K., Toriba, A., Tang, N., 2021. Exposure to atmospheric particulate matter-bound polycyclic aromatic hydrocarbons and their health effects: a review. Int. J. Environ. Res. Publ. Health 18 (4), 2177. https://doi.org/10.3390/ijerph18042177.

Zhang, W., Zhang, Z., Meng, H., Zhang, T., 2018. How does leaf surface micromorphology of different trees impact their ability to capture particulate matter? Forests 9 (11), 681. https://doi.org/10.3390/f9110681.

Zuzolo, D., Cicchella, D., Lima, A., Guagliardi, I., Cerino, P., Pizzolante, A., Thiombane, M., De Vivo, B., Albanese, S., 2020. Potentially toxic elements in soils of Campania region (Southern Italy): combining raw and compositional data. J. Geochem. Explor. 213, 106524 https://doi.org/10.1016/j.gexplo.2020.106524.